

Effective Rate of MISO Systems Over Fisher–Snedecor \mathcal{F} Fading Channels

Shuaifei Chen, Jiayi Zhang[✉], Member, IEEE, George K. Karagiannidis[✉], Fellow, IEEE,
and Bo Ai[✉], Senior Member, IEEE

Abstract—This letter investigates the effective rate (ER) of multiple-input single-output systems over both independent and identically distributed (i.i.d.) and independent and non-identically distributed Fisher–Snedecor \mathcal{F} fading channels with delay constraints. Novel closed-form expressions are derived for the ER of both aforementioned scenarios. Furthermore, for the i.i.d. case, asymptotic simple closed-form expressions for the ER in high- and low-signal-to-noise-ratios are provided. Physical insights about the impact of channel and system parameters on the ER are also revealed. An interesting finding is that the ER increases with the mean channel power, while it decreases with the delay factor. Finally, the correctness of the analytical results is validated through Monte Carlo simulations.

Index Terms—Fisher–Snedecor \mathcal{F} distribution, delay constraint, effective rate, MISO systems.

I. INTRODUCTION

THE performance of wireless communication systems can be improved by adopting multiple antennas at the transmitter, called as multiple input single output (MISO) systems. In this context, Shannon capacity has been investigated as a fundamental performance metric in several previous works. Alternatively to Shannon capacity the effective rate (ER) (or effective capacity) was proposed in [1] as a quality-of-service (QoS) metric, capable of taking the system's delay constraint into account. In [2], Zhang *et al.* studied the ER, when the channel is subject to $\kappa\text{-}\mu$ shadowed fading. Furthermore, Karatza *et al.* [3] considered the ER in multi-source and multi-destination cooperative networks over Rayleigh fading channels, while [4] conducted an analysis of the ER of a MISO system over several well-known fading channels, i.e., Rician, Nakagami- m , and Generalized- \mathcal{K} . However, these channels either model the shadowing by using the lognormal

Manuscript received August 29, 2018; revised October 10, 2018; accepted October 11, 2018. Date of publication October 16, 2018; date of current version December 10, 2018. This work was supported in part by the National Natural Science Foundation of China (No. 61601020), the Beijing Natural Science Foundation (Nos. 4182049 and L171005), the open research fund of National Mobile Communications Research Laboratory, Southeast University (No. 2018D04), Key Laboratory of Optical Communication and Networks (No. KLCN2018002), National Key Research and Development Program (No. 2016YFE0200900), and Major projects of Beijing Municipal Science and Technology Commission (No. Z181100003218010). The associate editor coordinating the review of this paper and approving it for publication was E. Radoi. (*Corresponding author:* Jiayi Zhang.)

S. Chen and J. Zhang are with the School of Electronic and Information Engineering, Beijing Jiaotong University, Beijing 100044, China, and also with the National Mobile Communications Research Laboratory, Southeast University, Nanjing 210096, China (e-mail: jiayizhang@bjtu.edu.cn).

G. K. Karagiannidis is with the Department of Electrical and Computer Engineering, Aristotle University of Thessaloniki, 54124 Thessaloniki, Greece (e-mail: geokarag@auth.gr).

B. Ai is with the State Key Laboratory of Rail Traffic Control and Safety, Beijing Jiaotong University, Beijing 100044, China (e-mail: aibo@ieee.org). Digital Object Identifier 10.1109/LCOMM.2018.2876426

distribution, which renders most statistics of interest analytically intractable, or require the evaluation of complex special functions.

More recently, a composite fading model named Fisher–Snedecor \mathcal{F} was proposed in [5], which shows accurate fit of experimental measurements for wireless body area networks (WBANs). Additionally, based on the experimental channel data provided therein, it was presented that the Fisher–Snedecor \mathcal{F} fits better in most of the cases, compared to Generalized- \mathcal{K} fading model. Importantly, its statistical characteristics are more tractable: Badarneh *et al.* [6] presented closed-form expressions for the sum of independent and non-identically distributed (i.n.i.d.) Fisher–Snedecor \mathcal{F} random variables (RVs), while in [7], the physical layer security of the Wyner's wiretap model in Fisher–Snedecor \mathcal{F} fading was investigated. However, to the best of the authors' knowledge, the ER of MISO systems over Fisher–Snedecor \mathcal{F} fading channels is still not available in the open technical literature.

Motivated by the above considerations, this letter studies the ER of MISO systems over both i.i.d. and i.n.i.d. Fisher–Snedecor \mathcal{F} fading channels. Novel closed-form formulas are derived, while in order to provide meaningful insights about the impact of the system and channel parameters on the ER, asymptotic simple and insightful closed-form expressions are derived. Based on these results, some useful guidelines for the design of MISO systems are provided.

II. SYSTEM MODEL

In this letter, a flat-fading MISO system is considered, where the transmitter is equipped with n_T antennas. The received signal at the receiver is given by

$$y = \mathbf{h}\mathbf{x} + n, \quad (1)$$

where \mathbf{h} is a channel fading vector and \mathbf{x} is the transmit vector. It is assumed that the transmit power P is equally allocated to each antenna, i.e., $\mathbb{E}\{\mathbf{x}\mathbf{x}^\dagger\} = (P/n_T)\mathbf{I}$, where $\mathbb{E}\{\cdot\}$ means expectation and \mathbf{I} is the unit matrix.

As proposed in [8], the MISO system can be considered as a queuing system over block fading channels, where the packets arrive according to a stationary service process. It is further assumed that the transmitter sends uncorrelated complex Gaussian signals with zero-mean and only the receiver has available channel state information [3], [4]. The ER is defined as [8, eq. (3)]

$$R(\rho, \theta) = -\frac{1}{A} \log_2 \left(\mathbb{E} \left\{ \left(1 + \frac{\rho}{n_T} \mathbf{h}\mathbf{h}^\dagger \right)^{-A} \right\} \right) \text{ bits/s/Hz}, \quad (2)$$

where ρ denotes the average signal-to-noise-ratio (SNR). Moreover, $A \triangleq \theta T B / \ln 2$ with θ being the decay factor, T is the block length and B is the system bandwidth.

Fisher-Snedecor \mathcal{F} distribution characterizes the simultaneous occurrence of multipath fading and shadowing, in which the root mean square (RMS) power of a received Nakagami- m signal is assumed to be subjected to variations induced by an inverse Nakagami- m RV. The probability density function (pdf) is given by [5, eq. (5)]

$$f_{\mathcal{F}}(\omega) = \frac{m^m (m_s \Omega)^{m_s} \omega^{m-1}}{B(m, m_s) (m \omega + m_s \Omega)^{m+m_s}}, \quad (3)$$

where $\Omega \triangleq \mathbb{E}\{\omega\}$ is the mean power, m and m_s denote the fading severity and shadowing parameters, and $B(\cdot, \cdot)$ is the beta function [9, eq. (8.384.1)].

III. I.I.D. FISHER-SNEDECOR \mathcal{F} FADING CHANNELS

A. Effective Rate

We assume that the elements of the channel vector, \mathbf{h} , follow i.i.d. Fisher-Snedecor \mathcal{F} distribution. From the definition, it can be readily observed that the sum of M i.i.d. Fisher-Snedecor \mathcal{F} RVs follows also a Fisher-Snedecor \mathcal{F} distribution, with parameters Mm , Mm_s and $M\Omega$. Thus, by using (3) along with some algebraic manipulations, the pdf of $\mathcal{H} = \sum_{\ell=1}^{n_T} |h_\ell|^2$ can be written as

$$f_{\text{i.i.d.}}(\omega) = \frac{m^{n_T m} (n_T m_s \Omega)^{n_T m_s} \omega^{n_T m - 1}}{B(n_T m, n_T m_s) (m \omega + n_T m_s \Omega)^{n_T(m+m_s)}}. \quad (4)$$

Substituting (4) into (2), and by using [9, eq. (3.197.1)], a closed-form expression for the ER over MISO i.i.d. Fisher-Snedecor \mathcal{F} fading channels is

$$\begin{aligned} R_{\text{i.i.d.}}(\rho, \theta) &= -\frac{1}{A} \log_2 \left[\frac{B(n_T m, A + n_T m_s)}{B(n_T m, n_T m_s)} \right. \\ &\quad \times {}_2F_1 \left(A, n_T m; A + n_T(m + m_s); 1 - \frac{\rho m_s \Omega}{m} \right) \Big], \end{aligned} \quad (5)$$

where ${}_2F_1(\cdot, \cdot; \cdot; \cdot)$ denotes the Gauss hypergeometric function [9, eq. (9.100)]. Note that this is a build-in function in most of the standard software packages (e.g., Matlab and Mathematica).

Although (5) is in closed-form, it includes special functions and thus, offers little insights into the physical impacts of the system and channel parameters on the ER. Therefore, it would be useful to investigate the ER in both high- and low-SNR regimes.

B. Asymptotic Effective Rate

In high-SNRs with $\rho \rightarrow \infty$, (2) can be written as

$$R(\rho, \theta) \approx -\frac{1}{A} \log_2 \left(\mathbb{E} \left\{ \left(\frac{\rho}{N_t} \mathbf{h} \mathbf{h}^\dagger \right)^{-A} \right\} \right). \quad (6)$$

Substituting (4) into (6) and using [9, eq. (3.194.3)], a simple closed-form expression for the ER at high-SNR can be derived as

$$\begin{aligned} R_{\text{i.i.d.}}^\infty(\rho, \theta) &= -\frac{1}{A} \log_2 \left(\frac{B(n_T m - A, n_T m_s + A)}{B(n_T m, n_T m_s)} \right) \\ &\quad + \log_2 \left(\frac{m_s \Omega}{m} \right) + \log_2 \rho. \end{aligned} \quad (7)$$

The diversity gain denotes the increase in the slope of $R_{\text{i.i.d.}}^\infty$ against the average SNR, ρ , which is evidently equal to 1 in this case. Also, it is worthwhile pointing out that the ER achieved as $\rho \rightarrow \infty$ is a monotonically increasing function of the number of antennas, n_T , and the shadowing parameter, m_s , due to the diversity contribution from the multi-antennas. Additionally, the shadowing of the RMS signal power in the Fisher-Snedecor \mathcal{F} fading channels does not exist when $m_s \rightarrow \infty$, and (7) reduces to Nakagami- m fading.

The ER of Fisher-Snedecor \mathcal{F} fading channels in the low-SNR regime, can be written in terms of the normalized transmit energy per information bit, i.e., E_b/N_0 , as [10]

$$R(E_b/N_0) \approx S_0 \log_2 \left(\frac{E_b/N_0}{E_b/N_{0\min}} \right), \quad (8)$$

where S_0 denotes the rate against the SNR slope, and $E_b/N_{0\min}$ is the minimum E_b/N_0 required for reliably communication at any nonzero rate. As mentioned in [10], S_0 and $E_b/N_{0\min}$ can be derived from the first and second derivatives of $R(\rho, \theta)$ as $\rho \rightarrow 0$ through

$$\frac{E_b}{N_{0\min}} \triangleq \frac{1}{R'(0, \theta)} \quad (9)$$

$$S_0 \triangleq -\frac{2 \ln 2 (R'(0, \theta))^2}{R''(0, \theta)}, \quad (10)$$

where $R'(0, \theta)$ and $R''(0, \theta)$ are given in [8, eqs. (16) and (17)].

Since $\mathbb{E}\{|h_\ell|^2\} = \Omega$, it is easy to obtain that $\mathbb{E}\{\mathbf{h} \mathbf{h}^\dagger\} = n_T \Omega$. With the help of [5, eq. (9)], the fourth moment of $|h_\ell|$ is given by

$$\mathbb{E}\{|h_\ell|^4\} = \left(\frac{m_s \Omega}{m} \right)^2 \frac{B(m+2, m_s-2)}{B(m, m_s)}. \quad (11)$$

Therefore,

$$\begin{aligned} \mathbb{E}\{(\mathbf{h} \mathbf{h}^\dagger)^2\} &= \sum_{\ell=1}^{n_T} \mathbb{E}\{|h_\ell|^4\} + \sum_{i=1}^{n_T} \sum_{j=1, j \neq i}^{n_T} E\{|h_i|^2 |h_j|^2\} \\ &= n_T \left(\frac{m_s \Omega}{m} \right)^2 \frac{B(m+2, m_s-2)}{B(m, m_s)} + n_T(n_T-1)\Omega^2. \end{aligned} \quad (12)$$

With the aid of (9) and (10), holds that

$$\frac{E_b}{N_{0\min}} = \frac{\ln 2}{\Omega} \quad (13)$$

$$\begin{aligned} S_0 &= -2 \left[A - \frac{(A+1)}{n_T} \right. \\ &\quad \times \left. \left(\left(\frac{m_s}{m} \right)^2 \frac{B(m+2, m_s-2)}{B(m, m_s)} + n_T - 1 \right) \right]^{-1}. \end{aligned} \quad (14)$$

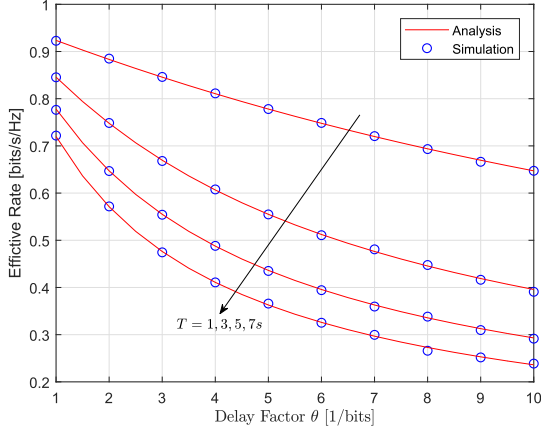


Fig. 1. Analytical and simulated ER against delay factor θ with different block length T for i.i.d. MISO Fisher-Snedecor \mathcal{F} fading ($n_T = 2$, $B = \ln 2$ Hz, $\rho = 0$ dB, $\Omega = 1$, $m = 2$, and $m_s = 30$).

Similar to the high-SNR case, the low-SNR slope S_0 increases with both n_T and m_s , while it monotonically decreases as A increases, that is, the delay factor θ , block length T , or system bandwidth B increases. Also note that $E_b/N_{0\min}$ is a decreasing function in the mean power Ω and is independent of other channel parameters (e.g., the fading severity parameter m and the shadowing parameter m_s) or the delay constraint θ .

IV. I.N.I.D. FISHER-SNEDECOR \mathcal{F} FADING CHANNELS

Let us consider a MISO system over i.n.i.d. Fisher-Snedecor \mathcal{F} fading channels. The pdf of the sum of the i.n.i.d. Fisher-Snedecor \mathcal{F} RVs is given by [6, eq. (5)]

$$\begin{aligned} f_{\text{i.n.i.d.}}(\omega) &= \frac{\omega^{\left(\sum_{\ell=1}^{n_T} m_\ell\right)-1}}{\Gamma\left(\sum_{\ell=1}^{n_T} m_\ell\right)} \left[\prod_{\ell=1}^{n_T} \left(\frac{m_\ell}{m_{s_\ell} \Omega_\ell} \right)^{m_\ell} \frac{\Gamma(m_\ell + m_{s_\ell})}{\Gamma(m_{s_\ell})} \right] \\ &\quad \times f_B \left(m_1 + m_{s_1}, \dots, m_{n_T} + m_{s_{n_T}}, m_1, \dots, m_{n_T}; \right. \\ &\quad \left. \sum_{\ell=1}^{n_T} m_\ell; \frac{-m_1}{m_{s_1} \Omega_1} \omega, \dots, \frac{-m_{n_T}}{m_{s_{n_T}} \Omega_{n_T}} \omega \right), \quad \omega \geq 0, \quad (15) \end{aligned}$$

where $f_B(\cdot)$ represents the Lauricella multivariate hypergeometric function [11, eq. (1.10.2)].

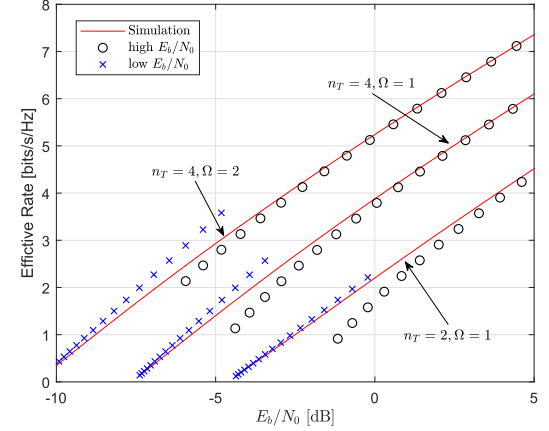


Fig. 2. High- and low- E_b/N_0 approximated and simulated ER against E_b/N_0 with different combination of n_T and Ω for i.i.d. MISO Fisher-Snedecor \mathcal{F} fading ($T = 1$ s, $B = \ln 2$ Hz, $\theta = 1$ 1/bits, $\Omega = 1$, $m = 2$, and $m_s = 30$).

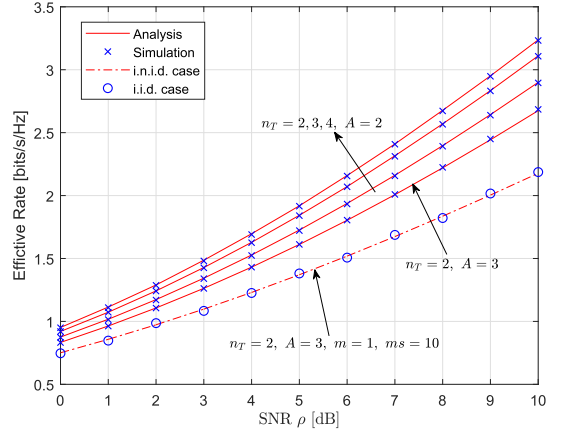


Fig. 3. Analytical and simulated ER against average SNR ρ with different combination of n_T and A for the case of i.n.i.d. MISO Fisher-Snedecor \mathcal{F} fading ($\Omega = 1$, $m = \{2, 1.5, 1.75, 2.5\}$, and $m_s = \{25, 30.5, 27.5, 35.75\}$).

Lemma 1: A closed-form expression for the ER in the i.n.i.d. case can be derived as in (16) at the bottom of this page, where $H_{p,q;\dots;\dots;\dots}^{0,n_1;\dots;n_{n_T};\dots;\dots;\dots}[\cdot|\dots]$ denotes the multivariate Fox H -function [12, Definition A.1].

Proof: Please see Appendix. ■

Note that, by rewriting the multivariate Fox H -function in (16) in the form of Mellin-Barnes integrals and using [9, eqs. (8.384.1) and (9.113)] and [12, Definitions. A.20 and A.31], the ER for the i.n.i.d. case can reduce to that for the i.i.d. case (5).

$$\begin{aligned} R_{\text{i.n.i.d.}}(\rho, \theta) &= -\frac{1}{A} \log_2 \left(\frac{1}{\Gamma(A)} \left[\prod_{\ell=1}^{n_T} \left(\frac{m_\ell}{m_{s_\ell} \Omega_\ell} \frac{n_T}{\rho} \right)^{m_\ell} \frac{1}{\Gamma(m_\ell) \Gamma(m_{s_\ell})} \right] \times H_{1,0:2,1;\dots;2,1}^{0,1:1,2;\dots;1,2} \left[\begin{array}{c} \frac{m_1}{m_{s_1} \Omega_1} \frac{n_T}{\rho} \\ \vdots \\ \frac{m_{N_T}}{m_{s_{N_T}} \Omega_{N_T}} \frac{n_T}{\rho} \end{array} \right] \right. \\ &\quad \left. \left(1 - A + \sum_{\ell=1}^{n_T} m_\ell; -1, \dots, -1 : (1 - m_1 - m_{s_1}, 1), (1 - m_1, 1); \dots; (1 - m_{n_T} - m_{s_{n_T}}, 1), (1 - m_{n_T}, 1) \right) \right) \\ &\quad - (0, 1); \dots; (0, 1) \quad (16) \end{aligned}$$

$$\begin{aligned}
R_{\text{i.n.i.d.}}(\rho, \theta) = & -\frac{1}{A} \log_2 \left(\frac{1}{\Gamma(A)} \left[\prod_{\ell=1}^{n_T} \left(\frac{m_\ell}{m_{s_\ell} \Omega_\ell} \frac{n_T}{\rho} \right)^{m_\ell} \frac{1}{\Gamma(m_\ell) \Gamma(m_{s_\ell})} \right] \frac{1}{(2\pi i)^{n_T}} \right. \\
& \times \left. \int_{c_1} \int_{c_2} \cdots \int_{c_{n_T}} \Gamma \left(A - \sum_{\ell=1}^{n_T} (m_\ell + s_\ell) \right) \left[\prod_{\ell=1}^{n_T} \Gamma(m_\ell + m_{s_\ell} + s_\ell) \Gamma(m_\ell + s_\ell) \Gamma(-s_\ell) \left(\frac{m_\ell n_T}{m_{s_\ell} \Omega_\ell \rho} \right)^{s_\ell} \right] ds_1 ds_2 \cdots ds_{n_T} \right). \quad (18)
\end{aligned}$$

V. NUMERICAL RESULTS AND DISCUSSION

In order to validate the theoretical analysis, we perform Monte-Carlo simulations by generating 10^5 independent Fisher-Snedecor \mathcal{F} channel realizations. The ER against delay factor ρ for the block length T is depicted in Fig. 1. A perfect agreement can be observed between the analytical results (5) and those obtained by Monte-Carlo simulations. As anticipated, the ER monotonically decreases as delay factor θ and block length T increases as well because the initial decay-rate of the MISO system is proportional to block length T [13]. Additionally, the gap between the curves is narrowing, when the corresponding block length T increases, which implies that the longer T is, the more pronounced its effect will be.

Fig. 2 illustrates the ER, along with its high- E_b/N_0 approximation (from (7)) by using the expression $E_b/N_0 = \rho/(n_T R(\rho, \theta))$, and its low- E_b/N_0 approximation, as in (8). It is readily concluded that better ER performance can be achieved by increasing the number of antennas n_T . Also, an increase in the average power Ω may get the ER large but leaves the required $E_b/N_{0\min}$ value unaffected. Moreover, the approximation of the ER is considerably tight for all the cases. It is worth mentioning that in the high- E_b/N_0 case, the accuracy is improved by larger values of n_T and S_0 , which is on the contrary with case in the low- E_b/N_0 .

In Fig. 3, we plot the analytical and simulated ER of MISO i.n.i.d. Fisher-Snedecor \mathcal{F} fading channels against average SNR ρ , with different combination of n_T and A . Moreover, the ER for i.n.i.d. case provided in (16) is verified to coincide with the i.i.d. case provided in (5), when the fading parameters are the same, i.e., $\Omega = 1$, $m = 1$, and $m_s = 10$. It can be observed that the ER is a monotonically decreasing function of A , which indicates that the delay factor θ is a deterioration of the ER. Note that a higher rate can be yielded by more number of antennas n_T . Furthermore, the gap between the corresponding curves narrows as n_T increases, which implies that the effect of n_T becomes less pronounced.

VI. CONCLUSIONS

In this letter, the impact of delay on the ER of MISO systems over Fisher-Snedecor \mathcal{F} fading channels is investigated. When no delay constraint is imposed, i.e., the delay approaches to infinity, the ER tends to the Shannon capacity. Novel closed-form expressions for the ER over both i.i.d. and i.n.i.d. \mathcal{F} fading channels are derived. To obtain physical insights, a simple closed-form expression for the ER at high-SNR regime was also presented. Additionally, tractable expressions are derived at low-SNR regime. The results are beneficial for the design of practical MISO systems.

APPENDIX

By employing [11, eq. (1.10.10)], (15) is written in the form of multiple Barnes-type contour integrals as [6, eq. (21)]

$$\begin{aligned}
f_{\text{i.n.i.d.}}(\omega) = & \left[\prod_{\ell=1}^{n_T} \left(\frac{m_\ell}{m_{s_\ell} \Omega_\ell} \right)^{m_\ell} \right] \omega^{\left(\sum_{\ell=1}^{n_T} m_\ell \right) - 1} \frac{1}{(2\pi i)^{n_T}} \int_{c_1} \int_{c_2} \cdots \\
& \int_{c_{n_T}} \frac{1}{\Gamma \left(\sum_{\ell=1}^{n_T} (m_\ell + s_\ell) \right)} \left[\prod_{\ell=1}^{n_T} \frac{\Gamma(m_\ell + s_\ell) \Gamma(-s_\ell)}{\Gamma(m_\ell) \Gamma(m_{s_\ell})} \right. \\
& \times \left. \Gamma(m_\ell + m_{s_\ell} + s_\ell) \left(\frac{m_\ell}{m_{s_\ell} \Omega_\ell} \omega \right)^{s_\ell} \right] ds_1 ds_2 \cdots ds_{n_T}. \quad (17)
\end{aligned}$$

Substituting (17) into (2), and with the aid of [9, eq. (3.194.3)], we can derive (18). The proof is completed by expressing (18) in terms of the multivariate Fox H -function as (16), which can be efficiently implemented in Matlab [14].

REFERENCES

- [1] D. Wu and R. Negi, "Effective capacity: A wireless link model for support of quality of service," *IEEE Trans. Wireless Commun.*, vol. 2, no. 4, pp. 630–643, Jul. 2003.
- [2] J. Zhang, L. Dai, W. H. Gerstacker, and Z. Wang, "Effective capacity of communication systems over $\kappa-\mu$ shadowed fading channels," *Electron. Lett.*, vol. 51, no. 19, pp. 1540–1542, Sep. 2015.
- [3] G. P. Karatza, K. P. Peppas, and N. C. Sagias, "Effective capacity of multisource multideestination cooperative systems under cochannel interference," *IEEE Trans. Veh. Technol.*, vol. 67, no. 9, pp. 8411–8421, Sep. 2018.
- [4] M. Matthaiou, G. C. Alexandropoulos, H. Q. Ngo, and E. G. Larsson, "Analytic framework for the effective rate of MISO fading channels," *IEEE Trans. Commun.*, vol. 60, no. 6, pp. 1741–1751, Jun. 2012.
- [5] S. K. Yoo, S. L. Cotton, P. C. Sofotasios, M. Matthaiou, M. Valkama, and G. K. Karagiannidis, "The Fisher-Snedecor \mathcal{F} distribution: A simple and accurate composite fading model," *IEEE Commun. Lett.*, vol. 21, no. 7, pp. 1661–1664, Jul. 2017.
- [6] O. S. Badarneh, D. B. Da Costa, P. C. Sofotasios, S. Muhamadat, and S. L. Cotton, "On the sum of Fisher-Snedecor \mathcal{F} variates and its application to maximal-ratio combining," *IEEE Wireless Commun. Lett.*, to be published.
- [7] O. S. Badarneh, P. C. Sofotasios, S. Muhamadat, S. L. Cotton, K. Rabie, and N. Al-Dhahir. (2018). "On the secrecy capacity of Fisher-Snedecor \mathcal{F} fading channels." [Online]. Available: <https://arxiv.org/abs/1805.09260>
- [8] J. Zhang, Z. Tan, H. Wang, Q. Huang, and L. Hanzo, "The effective throughput of MISO systems over $\kappa-\mu$ fading channels," *IEEE Trans. Veh. Technol.*, vol. 63, no. 2, pp. 943–947, Feb. 2014.
- [9] I. S. Gradshteyn and I. M. Ryzhik, *Table of Integrals, Series, and Products*, 7th ed. New York, NY, USA: Academic, 1980.
- [10] A. Lozano, A. M. Tulino, and S. Verd, "Multiple-antenna capacity in the low-power regime," *IEEE Trans. Inf. Theory*, vol. 49, no. 10, pp. 2527–2544, Oct. 2003.
- [11] A. M. Mathai and H. J. Haubold, *Special Functions for Applied Scientists*. New York, NY, USA: Springer, 2008.
- [12] A. M. Mathai, R. K. Saxena, and H. J. Haubold, *The H-Function: Theory and Applications*. Springer, 2009.
- [13] L. Liu and J.-F. Chamberland, "On the effective capacities of multiple-antenna Gaussian channels," in *Proc. IEEE ISIT*, Jul. 2008, pp. 2583–2587.
- [14] H. Chergui, M. Benjillali, and M.-S. Alouini. (2018). "Rician K -factor-based analysis of XLOS service probability in 5G outdoor ultra-dense networks." [Online]. Available: <https://arxiv.org/abs/1804.08101>